CFD INSTRACTION GUIDE TO SIMULATE TWO-PHASE FLOW SEPARATION IN A VERTICAL T-JUNCTION SEPARATOR

RAID AHMED MAHMOOD

Faculty of Health, Engineering and Sciences, University of Southern Queensland, Queensland, Australia
E-mail: raidalneamy@yahoo.com, Raid.Mahmood@usq.edu.au

Abstract - Two-phase flow separation has been investigated by many researchers due to its important role in the most industrial applications. In refrigeration and air conditioning systems, two-phase flow separation influence the system performance. So, many techniques have been used to separate liquid phase from gas-liquid two phase flow and consequently to improve a system performance. T-junction is one of the techniques that can be used to obtain effective two-phase separation. In order to investigate the two-phase flow separation in very simple way and obtain wide accurate range of results, computational work is the appropriate solution. Computational Fluid Dynamics (CFD) software is one of the most effective computational way that can be used to visualise two-phase flow separation and design two-phase flow separator. This paper presents an instruction of CFD simulation to predict and visualize the two-phase flow separation in vertical T-junction and a comparison between the CFD results with therelated experimental results to validate the CFD results. ANSYS 17.1 was used to carry out the simulation. The geometry of the T-junction was generated by the ANSYS modular design based on the dimensions of experimental test section, then lunched to the ANSYS meshing to generate a suitable mesh.

Keywords - Two-Phase Flow, Two-phase Separation, Vertical T-junction, ANSYS Fluent 17.1, Visualize Two-Phase Flow.

I. INTRODUCTION

In the two-phase flow experiments, parameters such as pressure, temperature and mass flow rate have an important effect on the experiment and can be measured relatively easily. However, when more details are required such as volume fraction distribution for liquid and gas phases respectively, experimental work is more difficult and expensive. Computational Fluid Dynamic (CFD) simulation offers an alternative approach. In CFD simulations, descretised version of the differential equations which model the two-phase flow behaviour are solved.

Within the CFD two-phase modelling options in ANSYS 17.1 FLUENT, there are three different models: Volume of fluid (VOF), Mixture model and Eulerian model. The most appropriate choice of these model is influenced by the flow regime to be simulated, and four categories can be easily identified: gas-liquid or liquid-liquid flows, gas-solid flows, liquid-solid flows and three-phase flows [1]. In the gas-liquid flow regime, there are different flow patterns such as bubbly flow, droplet flow, slug flow, stratified wavy flow and stratified flow [2]. Consequently, the first step towards CFD simulation of a multiphase problem is to determine which of the flow regimes describe the flow of the particular problem that needs to be simulated. Many numerical simulations of gas-liquid two-phase flow have used the Eulerian model in different geometries including sudden expansion [3] and flow in a horizontal tube [4] because it is more accurate than the VOF and Mixture models [3]. In the Eulerian approach, the liquid phase and vapour phase are both treated as a continuous phase by using the volume fraction for each phase [5]. Walvekar, Choong [4] conducted a numerical study using CFD Fluent version 6.2 to simulate three dimensional two-phase flow in a horizontal tube. Two immiscible liquids: oil and water were used as the working fluids. The horizontal pipe had a 0.024 m inside diameter and 9.7 m length and this geometry was used as the domain to simulate the two-phase flow. The Eulerian-Eulerian two-phase model with 0.001 s time steps were used to achieve transient simulation of the two-phase flow inside the horizontal pipe. Velocity inlet and pressure outlet were specified as a boundary conditions. The results were compared with the experimental results from other literature. The results revealed that the CFD was successful in simulating the two-phase dispersed liquid-liquid flows, and an average relative deviation between the simulations and the experiment of 3.41% was obtained for the oil holdup parameter.Zarrouk and Purnanto [6] reviewed recent research that utilises CFD for steam-water cyclone separator design. The study demonstrated that the CFD simulations provide insight to the two-phase behaviour and features that cannot be analysed from any empirical approach.

Indeed, CFD simulation has been used to optimize the geometry and predict the two-phase flow behavior such as sudden expansion Hwang and Pal [7] and Roul and Sahoo [3], bubble columme Delnoij, Kuipers [8] and Rampure, Buwa [9], cylinderical vessels Gandhi, Joshi [10], inclined pipe Dasari, Goshika [11], horizontal tube Walvekar, Choong [4], vertical and horizontal tubes Parvareh, Rahimi [12] and horizontal tubes Ekambara, Sanders [13]. Howvere, water two-phase flow was not considered.
This paper presents a CFD instruction to simulate water two-phase flow separation in a T-junnction and validation of the CFD results with experiments, using Eulerian-Eulerian two-phase model. ANSYS workbench with Fluent were used to carry out the

simulations and present the result using post processing. The simulation process starts with design modeller to creat a 3D vertical T-junction. Then, generat mesh by using ANSYS meshing and finally proceed the solution via ANSYS Fluent.

II. GEOMETRY GENERATION

In the present work, the design module of the ANSYS Workbench 17.1 was used to create the domain for the vertical T-junnction based on the experimental test section dimentions which are D=9 mm, L=200 mm and H=60 mm. The domain of the vertical T-junnction geometry was created in the 3D mode with exploitation of the symmetry plane as shown in Figure 1.

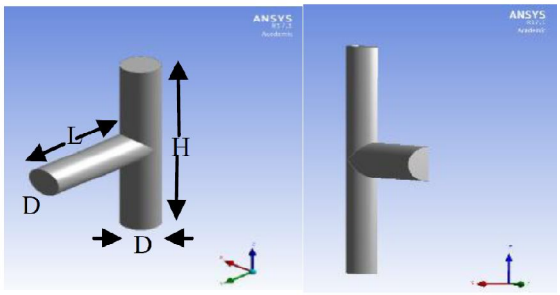

Fig. 1 Domain of the vertical T-junnction geometry.

III. MESH GENERATION

3.1 Mesh quality

The meshes created for the vertical T-junnction simulations were created from tetrahedral elements which has benefits such as reduced computational time and improved mesh quality for three dimensional domains of complex shapes [14]. The meshes were generated and optimized using Ansys Meshing. An unstructured grid was obtained using global and local sizing parameter after a series of tests. According to the Fluent user guide [5], obtaining good mesh quality will give accurate solutions and fast convergence.

The mesh quality can be represented by three factors namely, orthogonal quality, aspect ratio, and skewness value [15]. The orthogonal quality ranges from 0 to 1 and 0 represents low mesh quality. The minimum orthogonal quality should always be greater than or equal to 0.01 [5]. The aspect ratio is relevant to the wall function and should be small enough to allow the solution to capture the flow details near the wall [16]. The skewness value, which is inversely related to solution accuracy, should be small enough to minimize error in the solution [17]. For the meshe used in the present simulations, the orthogonal quality was 0.9 with a minimum value of 0.07, the aspect ratio was 3.56, and skewness value was 0.26. These values indicate that according to the established criteria, good mesh qualities were obtained and used in the present simulations.

3.2 Mesh independence study

The geometry of the vertical T-junnction was discretized into tetrahedral elements and in order to generate a fine mesh near the walls, the inflation method was used. Figure 2 illustrates the mesh of the vertical T-junnction. Four computational grids of 8500, 18000, 140000 and 280000 were used to investigate the grid independence in the vertical T-junnction case. Figure 3 shows the liquid volume fraction distribution in the inlet of the vertical T-junction at 100 mm from inlet for different mesh densities. The red area represents the liquid film at the bottom of the pipe and the transitional colours between the red and blue represents the interface between the phases. The figure 3 also illustrates the significant effect of the different element numbers on the resolution of the interface of two-phase flow. It can be seen that there is no significant change in the liquid volume fraction and the smoothing of interface between the liquid and vapour when the mesh number increased beyond 140000.

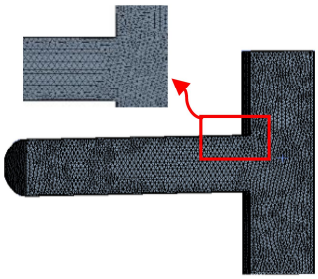

Fig. 2 Vertical T-junnction mesh with inflation near the walls for the 140000 element mesh case.

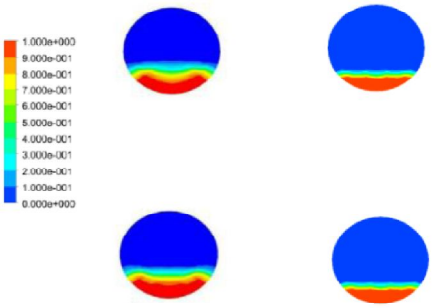

Fig. 3 Assessment of grid independence showing liquid volume fraction contours for different element numbers in the inlet of the T-junction at developed region, (100 mm from the inlet of the T-junction for operating condition $\dot{m}$= 10.2 g/s, x=5.2 %)

IV. BOUNDARY CONDITION

In order to generate simulations consistent with the experimental data, the same operating conditions were used in the CFD simulation. Water was used as the working fluid. At the inlet, the liquid droplet size

was selected according to the expansion device design which has 400 holes with 0.3 mm diameter, so the liquid droplet diameter was selected to be 300 µm. On the assumption that homogeneous adiabatic flow is formed directly after the expansion device, the velocity at the inlet of the horizontal tube can be calculated based on the homogeneous void fraction [18]. The inlet liquid velocity can be calculated from

$$u_l = \frac{m_l}{\rho_l A(1-\alpha_{hg})} \quad (1)$$

Where the A is the total cross section area of the horizontal pipe, ρ_l is the liquid density, $\dot{m}l$ is the liquid mas flow rate and α_g is the gas void fraction which can be calculated from

$$\alpha_{hg} = \left[1 + \left(\frac{1-x}{x}\right)\left(\frac{\rho_g}{\rho_l}\right)\right]^{-1} \quad (2)$$

Similarly, the inlet gas velocity at the inlet can be calculated from

$$u_g = \frac{m_g}{\rho_g A \alpha_{hg}} \quad (3)$$

Where the ρ_g is the gas density, $\dot{m}g$ is the gas mass flow rate. The inlet boundary condition was specified as uniform velocity distribution for each phase at the inlet of the vertical flash tank. A pressure outlet was used for the outlet boundary condition. The no slip wall was applied for the wall boundary.

Selecting primary and secondary phases depends on the two-phase flow pattern, in the present study the liquid was identified as primary phase and the gas was the secondary phase. Then, boundary conditions can be set up after selecting the primary and secondary phases. Velocity inlet was applied for the inlet two-phase, while pressure outlet and no slip were applied for the outlet flow and separator wall respectively. The boundary conditions were obtained from the experiments.

V. CFD SOLUTION SETUP

In this study, double precision was used in the two-phase flow simulation to obtain an accurate solution. However, the solution of the double precision is slower than single precision [19]. Figure 4 shows the set up window of the Fluent launcher. Serial solver manages file input and output, data storage, and flow field calculations using a single solver process on a single computer, while parallel solver allows you to compute a solution by using multiple processes that may be executing on the same computer, or on different computers in a network [5]. Therefore, serial solver was selected for the local machine. From the general task page, the solver type pressure-Based and velocity formulation Absolute have been selected. Steady state has been selected from time section. Figure 5 shows the details of set up. Gravity has also been activated on the Y-axis direction to consider the gravity effect on the two-phase flow.

The second-order scheme was used to discretise the governing equations including mass and momentum energy in addition to the turbulence transport and two-phase flow model. Figure 6 shows flow chart of the numerical simulation steps.

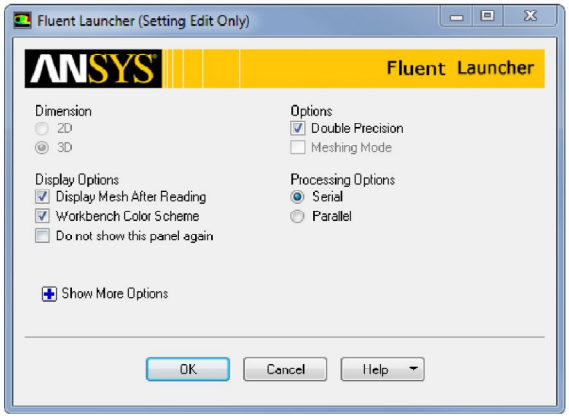

Fig. 4 Fluent launcher two-phase flow CFD setup.

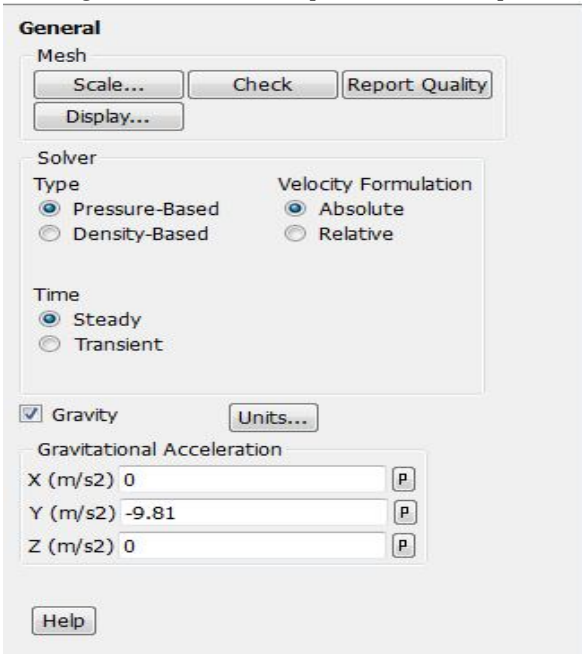

Fig. 5 General task page of two-phase CFD setup.

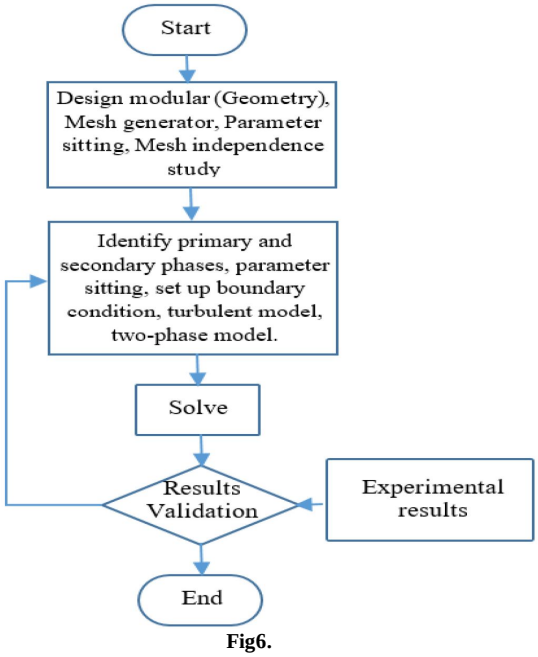

Fig6.

VI. EXPERIMENTAL APPARATUS

The experimental apparatus was designed and built in such a manner to investigate the two-phase liquid separation efficiency which is related to the present study. The experimental apparatus consisted of the test section (vertical T-junction separator), vacuum pump, condenser, heat exchanger and expansion device. Measurements including video recordings were used to ascertain the temperature, pressure and mass flow rate in the vertical T-junction separator. All the measurement sensors were connected to the data acquisition equipment. As the working fluid was water in this study, a special design was used for the expansion device. VisiJet crystal (EX 200 material) was used to fabricate the expansion device using a 3D printer model ProJetTM SD & HD 3500. The VisiJet material has a limited maximum working temperature of around 65 ^{O}C. The expansion device was designed to provide a uniform two-phase flow distribution across the inlet port of the vertical T-junction separator.

VII. RESULTS AND DISCUSSION

In order to determine the liquid height according to the liquid volume fraction definition and compare it with the experimental data, transverse vertical plane at 1665 mm from the inlet is defined in the CFD simulations.

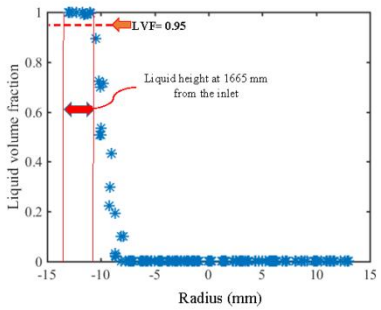

Fig. 7 Liquid height identification on the central vertical plane of the pipe at 1665 mm from the inlet, according to the liquid volume fraction definition for $\dot{m}$ =13.1 g/s, x=5.3.

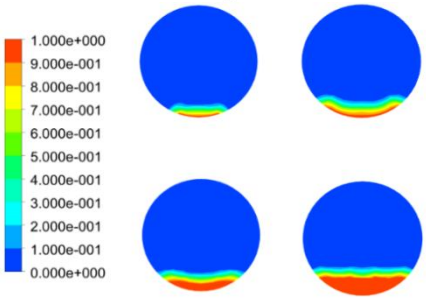

Figure. 8 Liquid volume fraction on the vertical planes perpendicular to the flow direction at 1665 mm from the inlet for the different operation conditions.

Figure 7 illustrates the liquid volume fraction distribution at this location and includes the liquid height definition which is illustrated by the distance between the two vertical lines. The liquid height is defined by the zone in which the liquid volume fraction is greater than 0.95, an approach consistent with that adopted for the expansion region. The simulated liquid volume fraction in the fully developed region for the different operating conditions is shown in Figure 8. It is seen that the mass flow rate has a significant effect on the liquid height.

Separation Efficiency And Validation

In order to validate the CFD results with the experimental results, variation of the liquid separation efficiency with the inlet mass velocity for different operating conditions of the vertical separator is presented and compared with the experimental results in Figures 9. Generally, the results revealed that the liquid separation efficiency increased gradually as a result of increasing the inlet mass flow rate. The trend of the numerical results is similar to that in the experimental results and good agreement was observed between the numerical and experimental results. However, the simulations consistently underestimate the separation efficiency by an amount that varies between about 0.01 and 0.02. For example, in the highest separation efficiency, which was achieved at an inlet mass velocity of 44.23 kg/m^2.s, the experiment gave $\acute{\eta}_L$= 0.96 whereas the simulation indicated 0.94.

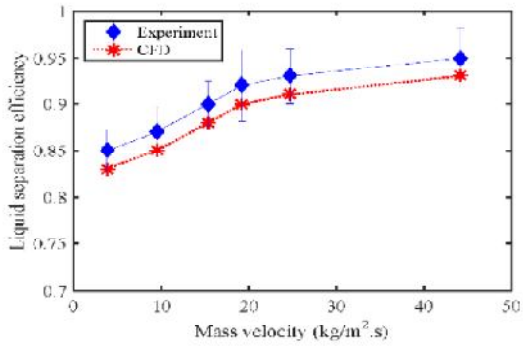

Fig. 9 Numerical and experimental results for liquid separation efficiency.

As the mass flow rate at the inlet and liquid outlet of the vertical tank were measured using mass flow meters, uncertainty of the mass flow rates measurement at the inlet and liquid outlet of the vertical T-junction separator directly affects uncertainty in the liquid separation efficiency. In the Figures 9, the error bars denote the estimated uncertainty of the efficiency due to the mass flow rate measurements from the experimental data. The highest value of the uncertainty in efficiency in the experiments for the vertical tank was about ± 0.058.

ACKNOWLEDGMENTS

I acknowledge the University of Southern Queensland for providing the equipment and laboratory for this research

REFERENCES

[1] Hu, H. and Y.F. Cheng, Modeling by computational fluid dynamics simulation of pipeline corrosion in CO 2-containing oil-water two phase flow. Journal of Petroleum Science and Engineering, 2016. 146: p. 134-141.
[2] Roman, A.J., et al., Flow pattern identification of horizontal two-phase refrigerant flow using neural networks. International Communications in Heat and Mass Transfer, 2016. 71: p. 254-264.
[3] Roul, M.K. and L.K. Sahoo, CFD modeling of pressure drop caused by two-phase flow of oil/water emulsions through sudden expansions. 2012. 2(6): p. 1047-1054.
[4] Walvekar, R.G., et al., Numerical study of dispersed oil–water turbulent flow in horizontal tube. Journal of Petroleum Science and Engineering, 2009. 65(3): p. 123-128.
[5] FLUENT, A., 14.5, Theory Guide; ANSYS. Inc., Canonsburg, PA, 2012.
[6] Zarrouk, S.J. and M.H. Purnanto, Geothermal steam-water separators: Design overview. Geothermics, 2015. 53: p. 236-254.
[7] Hwang, C.-Y.J. and R. Pal, Flow of two-phase oil/water mixtures through sudden expansions and contractions. Chemical Engineering Journal, 1997. 68(2): p. 157-163.
[8] Delnoij, E., J. Kuipers, and W. Van Swaaij, Computational fluid dynamics applied to gas-liquid contactors. Chemical engineering science, 1997. 52(21): p. 3623-3638.
[9] Rampure, M.R., V.V. Buwa, and V.V. Ranade, Modelling of Gas-Liquid/Gas-Liquid-Solid Flows in Bubble Columns: Experiments and CFD Simulations. The Canadian Journal of Chemical Engineering, 2003. 81(3-4): p. 692-706.
[10] [10] Gandhi, M.S., J.B. Joshi, and P.K. Vijayan, Study of two phase thermal stratification in cylindrical vessels: CFD simulations and PIV measurements. Chemical engineering science, 2013. 98: p. 125-151.
[11] Dasari, A., et al., CFD Simulation and Validation of Interfacial Morphology of Viscous Oil-Water Flow through Upward Inclined Pipe. Lubricating oil, 2014. 889: p. 0.107.
[12] Parvareh, A., et al., CFD and ERT investigations on two-phase flow regimes in vertical and horizontal tubes. International Communications in Heat and Mass Transfer, 2010. 37(3): p. 304-311.
[13] Ekambara, K., et al., CFD Modeling of Gas-Liquid Bubbly Flow in Horizontal Pipes: Influence of Bubble Coalescence and Breakup. International Journal of Chemical Engineering, 2012. 2012: p. 20.
[14] Vallée, C., et al., Experimental investigation and CFD simulation of horizontal stratified two-phase flow phenomena. Nuclear Engineering and Design, 2008. 238(3): p. 637-646.
[15] Rudolf, P., Connection between inlet velocity field and diffuser flow instability. Journal of Applied and Computational Mechanics, 2009. 3: p. 177-184.
[16] Lanzafame, R.a.M., S and Messina, M, Wind turbine CFD modeling using a correlation-based transitional model. Renewable Energy, 2013. 52: p. 31-39.
[17] Ali, Z.a.T., Paul G and Shahpar, Shahrokh, Optimal mesh topology generation for CFD. Computer Methods in Applied Mechanics and Engineering, 2017. 317: p. 431-457.
[18] El Hajal, J., J.R. Thome, and A. Cavallini, Condensation in horizontal tubes, part 1: two-phase flow pattern map. International Journal of Heat and Mass Transfer, 2003. 46(18): p. 3349-3363.
[19] Wang, W. and J. Li, Simulation of gas–solid two-phase flow by a multi-scale CFD approach—of the EMMS model to the sub-grid level. Chemical Engineering Science, 2007. 62(1-2): p. 208-231.

★★★